Scanning electron microscopy and EDX spectroscopy of commercial swabs used for COVID-19 lateral flow testing

Manuel Aparicio-Alonso[1*], Verónica Torres-Solórzano[2], José Francisco Méndez Contreras[3], Karina Acevedo-Whitehouse[2*]

[1] Centro Médico Jurica, Querétaro, México.
[2] Facultad de Ciencias Naturales, Universidad Autónoma de Querétaro, México.
[3] Retired Chemical Engineer. Independent Researcher

[*]Correspondence: draparicioalonso@gmail.com, karina.acevedo.whitehouse@uaq.mx

Abstract

The chemical composition of COVID test swabs has not been examined beyond the manufacturers' datasheets. Given the unprecedented demand for swabs to conduct rapid lateral flow tests and nucleic acid amplification tests, which led to mass production, including 3-D printing platforms, it is plausible that manufacturing impurities could be present in the swabs and, if so, could pose a risk for human health. We used scanning electron microscopy and energy dispersive X-ray (EDX) spectroscopy to examine the ultrastructure of five assorted brands of COVID test swabs, and to identify and quantify their chemical elements. We detected unexpected elements, including transition metals, such as titanium and zirconium, as well as aluminium, silicon, and fluorine. The amount of some of the detected elements is close to reported toxicological thresholds for inhalation routes. Experimental studies have shown that detrimental effects of the unexpected chemical elements include moderate to severe inflammatory states in the exposed epithelium as well as proliferative changes. Given the massive testing still being used in the context of the COVID pandemic, often as requisites for travelling, attending universities, or as mandatory work policies, we urge caution in continuing to recommend repeated and frequent testing, particularly of healthy, non-symptomatic, individuals.

Keywords: nasopharyngeal swabs, COVID, energy dispersive X-ray spectroscopy, scanning electron microscopy, transition metals, metalloids, titanium, zirconium, aluminium, silicon

Introduction

Methods to diagnose infectious disease increasingly depend on rapid tests that allow the detection of specific antigens or antibodies against a specific antigen. It is beyond the scope of this paper to discuss the validity of equating the detection of a protein fragment to diagnosing disease. Regardless of the nuances in such assumptions, these rapid tests are currently considered central for disease diagnosis. In the context of the COVID-19 (herein, COVID) pandemic, nucleic acid amplification tests (NAAT) and lateral flow tests (LFT), both based on nasopharyngeal swabbing, are the official methods for diagnosing COVID, and since their authorization at the start of 2020, thousands of millions of tests have been performed.

According to Our World in Data (accessed December 15th, 2022), between January 1st 2020 and December 16th 2022, 5,073,521,930 COVID tests have been performed, and this amount does not include the home tests that can be purchased in many countries and that are not informed to the health authorities, particularly when negative. The demand for such large-scale testing for COVID, unsurprisingly, could not be met by ordinary manufacturing of commercial nasopharyngeal swabs.[1] This led to mass production of swabs across various established and emerging manufacturers, and even to the 3-dimensional (3D) printing of nasopharyngeal swabs.[2,3] It is plausible that owing to the unprecedented speed of manufacturing and to the novel technological approaches to do so, impurities could realistically be present in the swabs used for mass testing. In the European Union, production, and commercialization of swabs for diagnostic purposes requires a *Conformité Européenne* (CE), certificate, which confirms that the manufacturer meets the minimum criteria for safety and environmental protection, in accordance with the provisions of Directive 93/42/EEC (14 June 1993) and Regulation 2017/745 (5 April 2017). However, to the best of our knowledge the technical datasheets for the COVID nasopharyngeal swabs do not provide any information on the presence, or maximum permitted amounts of microscopic and nanoscopic elements.

In terms of their fabric, there are different types of swabs used for diagnostic purposes, including cotton, rayon, polyester, nylon, polyurethane and foam.[4–6] Physical and chemical properties of the fabric can influence sample adhesion and release,[7] owing to structural variations of the fabric.[8] Interestingly, an unbiased search of the literature reveals that not a single study on the composition of the COVID test swabs has been published. Nearly all of the published studies on nasopharyngeal swabs used for COVID testing have examined their performance.[7,9–11] and we found only one review paper that compared the physical properties of different swab fabrics.[12]

It is sensible to know the components of COVID swabs if we wish to be confident about their safety; particularly as the testing method demands insertion of the swab into the delicate nasopharyngeal anatomy. Furthermore, despite nasopharyngeal swabs being graded as class I medical devices,[13] and as such, considered low risk, swabbing complications are known to occur, albeit at a low frequency.[14] There are now published reports of complications stemming from COVID testing, that range from mild (i.e. discomfort, pain or bleeding), to moderate (i.e. ethmoidal silent sinus syndrome), and serious, including breaches of the anterior skull base associated with a risk of meningitis.[13,15–19] If impurities are present in the swab, the risk of exposing the nasopharyngeal epithelium, or, even, the bloodstream to these should not be ignored, particularly considering repeated exposure from recurrent sampling.

This study is a first report of the ultrastructure and chemical composition of five brands of COVID testing swabs.

Methods

We analysed two specimens of each of five different brands of nasopharyngeal swabs, of brands iHealth®, Puritan HydraFlock®, MANTACC®, Nasal Swab and FLOQSwabs® (Table 1). In addition, one specimen of two cotton swab brands commonly used as applicators and for bacterial transport were included as control swabs (not COVID-test swabs). In order to determine

swab morphology, scanning electron microscopy (SEM) images of the tip, lateral walls and base of the swabs were taken using a EVO50 (Carl Zeiss AG) SEM with variable pressure and an acceleration voltage of 20 kV and with magnification at 30 x and 100 x. Resolution was 200 µm and 100 µm. In order to identify the chemical composition of the swabs' fabric, we performed X-ray spectroscopy using SE1, BSD, and EDX detectors. All analyses were conducted at the Laboratory of Microscopy of the School of Natural Sciences of the Autonomous University of Queretaro (Mexico). All swabs were handled with sterile gloves, and the packages were opened with extreme care immediately before the SEM and EDX spectroscopy to avoid potential contamination of the swabs.

Table 1. Swabs that were examined in this study.

Brand	Fabric	Purpose	Sterilization	CE	Manufacturer	Lot number
iHealth®	Foam	NP	OE	No	iHealth Labs,Inc	20211213
Puritan HydraFlock®	Nylon flocked	NP	OE	Yes	Puritan Med Products	(10) 50173
Nasal Swab	Nylon flocked	NP	OE	Yes	CM LAB SAS	20201221
MANTACC®	Nylon	NP	OE	Yes, 0197	Miraclean Technology Co., Ltd	2021120864
FLOQSwabs ®	Nylon	NP	OE	Yes, 0123	COPAN	2010482
Aplicador	Cotton	A	OE	Yes	DM Productora S.A. de C.V.	070319
Transystem®	Cotton	T	R	Yes, 0123	COPAN	211701500

NP, Nasopharyngeal; T, transport; A, applicator; EO, ethylene oxide; R, radiation, CE, Conformité Européenne.

We weighed the head of a duplicate of each of the swab brands to determine their mass (to the nearest 0.001 g). This data was used to convert the percentage of each element detected by EDX spectroscopy to mg, by way of a direct mathematical proportion, taking into account the sum of the percentage of each element detected (range: 99.02% to 99-79%) as the total percentage.

Results

SEM images of the swabs are shown in Figure 1. Two of each of the different swab brands made of foam (1), nylon (4) and one of each cotton control swabs were examined by SEM. The integrity of the head appeared intact, without evidence of biological (fungal spores or bacteria), contamination. However, the COPAN nylon swab showed crust-like elements surrounding the fibres. The iHealth foam swabs (Fig. 1A) revealed an alveolus-like network structure of varying diameters. In the nylon swabs (Fig. 2B-2E), individual fibres of homogeneous length were observed protruding from the head of the swab, more noticeably so in the Puritan HydraFlock swab, where each fibre had split or unravelled ends (Fig. 1B), similar to the head of a Hydra,

which is where the swab brand derives its name. In the cotton swabs (Fig. 2F, 3G), fibres were disorganized and with varying length, wrapped in one single direction.

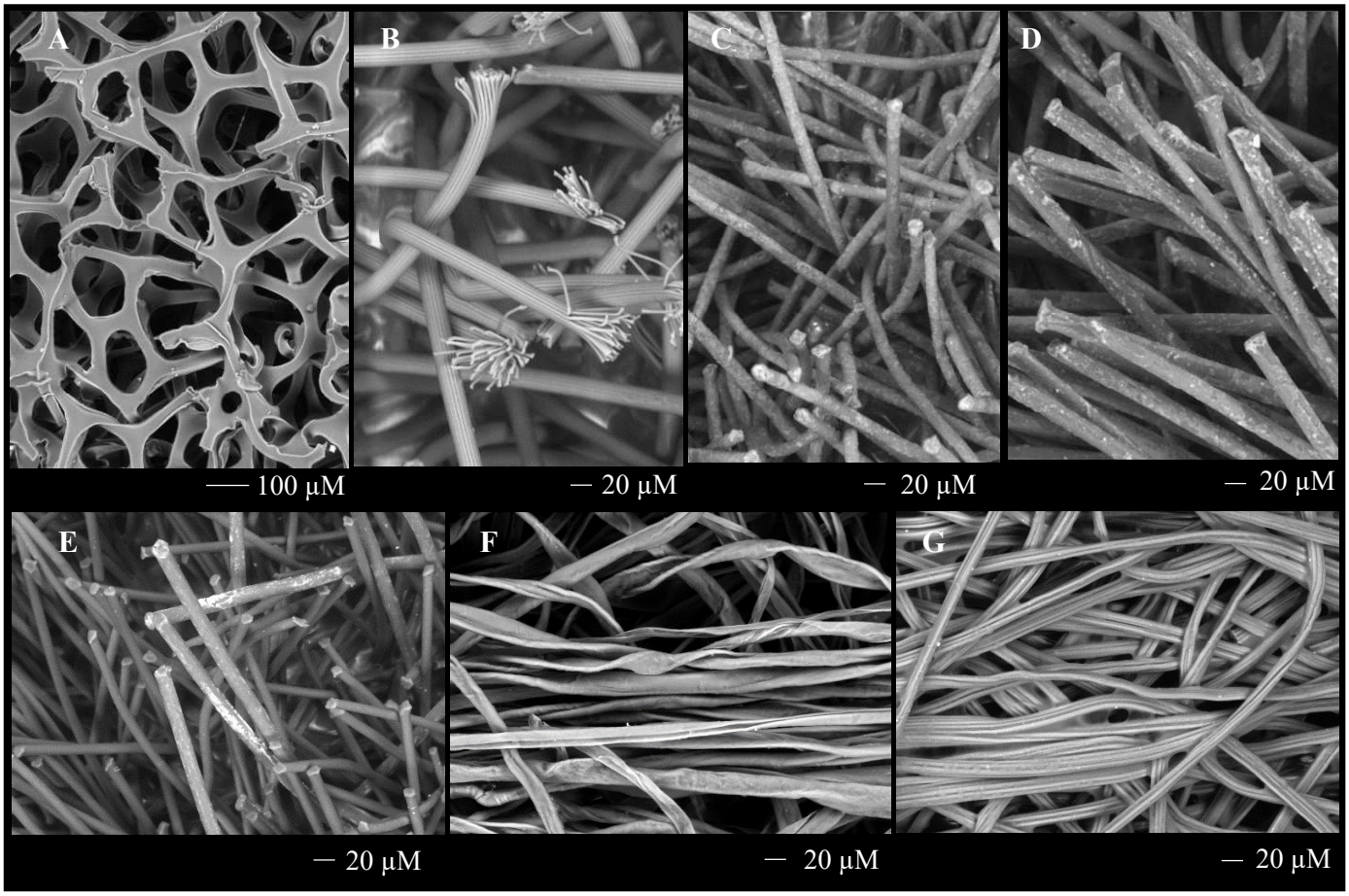

Figure 1. Scanning electron micrographs of different materials and structures of A) foam swab (iHealth), B) nylon-flocked swab (Puritan), C) nylon-flocked swab (CM LAB), D) nylon swab (Miraclean), E) nylon swab (COPAN), F) cotton swab used for generic applications (DM Productora) and G) cotton swab used for bacterial transport (COPAN). Magnification was 300 X except for panel A, which is 100X.

Nine elements were detected in the EDX spectroscopy analysis of the swabs (Table 2 and Figure S1 in Supplementary Material), of which the most abundant were carbon (48.97% to 63.84%) and oxygen (23.24% to 50.31%). Nitrogen was detected in only four of the swab brands (ranging from 4.75% to 10.26%), and we detected fluorine (F), silicon (Si), titanium (Ti), strontium (Sr), aluminium (Al) and zirconium (Zr) at low percentages (0.5%-1.2%). Of these, silicon, titanium, and strontium were not detected in the sterile cotton swabs used for generic applications, as applicators and for transport of bacterial samples.

Table 2. X-ray spectroscopy analysis of the swabs. The table shows the percentage of each chemical element identified for each swab, and the total percentage of identified elements. We include the estimation of the amount (mg) of each element detected, according to the swab head mass and percentage detected in the analysis.

	iHealth®	Puritan® HydraFlock®	Nasal Swab	MANTACC®	FLOQSwabs®	Aplicador	Transystem®
Swab head mass	0.0471 g	0.0539 g	0.0468 g	0.0385 g	0.0371 g	0.0501 g	0.0575 g
Carbon	57.99 %	62.43 %	53.13 %	59.60 %	63.84 %	48.97%	50.65%
	27.45 mg	33.77 mg	25.04 mg	23.17 mg	23.76 mg	24.59 mg	29.32 mg
Oxygen	33.51 %	36.82 %	36.29 %	29.22 %	23.24 %	50.31 %	46.78 %
	15.86 mg	19.92 mg	17.10 mg	11.36 mg	8.65 mg	25.26 mg	27.08 mg
Nitrogen	8.02 %	-	4.83 %	4.75 %	10.26 %	-	-
	3.79 mg	-	2.28 mg	1.85 mg	3.82 mg	-	-
Fluoride	-	0.52 %	0.53 %	-	-	0.50 %	0.57 %
	-	0.28 mg	0.25 mg			0.25 mg	0.33 mg
Silicon	-	-	4.18 %	3.79 %	0.54 %	-	-
	-	-	1.97 mg	1.47 mg	0.20 mg	-	-
Titanium	-	-	-	0.78 %	0.60 %	-	1.34 %
	-	-	-	0.30 mg	0.22 mg	-	0.78 mg
Zirconium	-	-	-	-	1.21 %	-	-
	-	-	-	-	0.45 mg	-	-
Strontium	-	-	-	0.87 %	-	-	-
	-	-	-	0.34 mg	-	-	-
Aluminium	-	-	0.62 %	-	-	-	-
	-	-	0.29 mg		-	-	-
Total	99. 52 %	99. 64 %	99.32 %	99.02 %	99.70 %	99.79 %	99.34 %

Discussion

Having knowledge about the chemical composition of the fabric and potential manufacturing impurities or by-products present in nasopharyngeal swabs that are being so frequently used for COVID testing of humans and, even, animals[20–22] is essential to ensure that potential health problems are minimized. Here, we analysed the chemical composition and ultrastructure of five brands of COVID testing swabs.

Hydrogen atoms are not detectable by X-ray spectroscopy,[23] but the majority of the elements detected, carbon, oxygen and nitrogen, concur with what is expected to find when analysing the composition of biopolymers and synthetic polymers. Specifically, cotton, rayon and polyester polymers are formed by carbon, hydrogen, and oxygen, with cotton and rayon having the formula $(C_6H_{10}O_5)_n$ [24] and polyester $(C_{10}H_8O_4)$[25]. Nylon polymers in turn, are formed by carbon, hydrogen, oxygen and nitrogen, $(C_{12}H_{22}N_2O_2)_n$[26] and foam swabs are made of high density polyurethane elastomers formed by diols (HO-R-OH) and diisocyanate (NCO-R'-NCO).[27] However, in addition to those expected elements, we found evidence of metalloids (silicon), transition metals (titanium and zirconium), post-transition metals (aluminium), and alkaline earth metals (strontium), none of which are indicated in the technical datasheet of the manufacturers. We also found evidence of traces of fluorine in two of the examined brands.

Evidently, it is the dose that makes the poison, and the unexpected elements detected represented a small percentage of the total elements identified by the EDX spectroscopy (see Table 2), a technique which allowed us to estimate the mass of each detected element in the swab head. Their presence, and estimated amount, in the swabs certainly warrants a discussion in terms of their potential impact to human health, particularly given the high number of tests that many people are undergoing, which could potentially lead to bioaccumulation of these elements in the body from repeated exposure. The bioaccumulation of aluminium,[28,29] and fluoride[30] are well recognized phenomena, although accumulation is highly dose-dependent.[31,32] Less studied is the bioaccumulation of transition metals in humans. However, experimental studies have shown that titanium nanoparticles can indeed accumulate in tissues[33,34] following contact with epithelia[35] even at low concentrations, and zirconium oxide (ZrO_2), commonly used in biomedical and dentistry applications,[36,37] has shown evidence of bioaccumulation in aquatic animals after environmental exposure of low concentrations.[38] Silicon dioxide nanoparticles (n-SiO_2), one of the most commonly used nanomaterials in biomedicine, pharmaceutical manufacturing, cosmetics[39–41] increasingly is being released into the environment and there is experimental evidence that it accumulates in the food chain.[42,43] Under the precautionary principle of medicine, it would be wise to assume that these nanoelements, detected in the COVID test swabs, could be accumulated in human tissues.

The biological impact of the detected elements to human cells also warrants a careful discussion. We will start by addressing the presence of fluorine, detected in two of the five brands of nasopharyngeal COVID test swabs as well as in the two sterile cotton swabs used as controls. According to the Agency for Toxic Substances and Disease Registry (ATSDR) of the Health and Human Services Department of the US, fluorine is soluble fluoride, and is a naturally occurring, widely distributed element and a member of the halogen family. The elemental form of fluorine,

is extremely reactive, and when in contact with water, forms fluorides and hydrofluoric acid.[44] Various studies have shown that fluoride can induce oxidative stress, deregulate cellular redox potential and lead to mitochondrial damage, promote endoplasmic reticulum stress and alter gene expression.[45] Studies on mice have shown that pre and perinatal exposure to fluoride can lead to neurobehavioral alterations, oxidative stress in the brain, and alteration of cholinergic and glutamatergic enzymes.[46] According to the US Environmental Protection Agency, the no observed adverse effect level (NOAEL) of fluoride is 1 ppm (converted to 0.06 mg/kg/day; https://iris.epa.gov/static/pdfs/0053_summary.pdf). If two swabs were used consecutively on a 12-month old child weighing less than 10 kg, the amount of fluorine detected in the COVID test swabs (average: 0.27 mg) would be close to the daily NOAEL. Evidently, we have no way of knowing how much of the fluoride in the swabs would actually be transferred to the nasopharyngeal epithelium following contact with the humid mucosa, but given the amount detected, future studies should aim to examine trace amounts of fluoride in the nasopharyngeal epithelium following swabbing.

Aluminium was only detected in one of the COVID test swabs, at a low percentage (0.62%, representing 0.29 mg). It is possible that its presence relates to the manufacturing process of that particular swab brand (Nasal swab) or to the presence of an unintended contaminant during packing of the swabs. Analysis of more samples would be necessary to establish whether it is indeed a component of this brand, or its finding was fortuitous. It could be argued that if it were established that this brand of COVID test swab contains traces of aluminium, the amount present is lower than the LOAEL of 26 mg/kg/day (oral route of administration[47]), making it unlikely that there would be any harmful effect from exposure. However, nasal exposure to aluminium salts (in rats) has shown that even small doses (10 µg) can lead to limited damage in the olfactory epithelium and detectable levels of aluminium in the olfactory bulb, increasing with increasing exposure.[48] Neurotoxicity of aluminium via inhalation has been studied and tends to be associated with higher doses; however, nasal instillation of rats with even low amounts (as low as 1 mg/kg) of Al_2O_3, revealed dose-dependent inflammation and alveolar–capillary barrier permeabilization after exposure.[49] Effects are likely due to the fact that aluminium can penetrate cell membranes in the site of exposure and also travel via the bloodstream and thus enter other cells, where it binds to proteins and enzymes, modulating cytokine expression.[50,51.] If this were to occur similarly following exposure to aluminium in the swabs, susceptible people could plausibly experience overexpression of cytokines in the nasopharyngeal mucosa,[52] similar to what has been described for aluminium adjuvants in nasal vaccines.[53]

Silicon was another unexpected finding in three of the five COVID test swab brands, with amounts varying from 0.20 to 1.97 mg. Data on the lowest estimated cumulative exposure range that has been reported in the literature is established for silica, a common oxide form of silicon, at <0.2 mg/m^3/year,[54] equivalent to up to 0.2 mg/kg/year. If we consider the highest value of silicon detected in one of the COVID test swab brands here analysed, undergoing seven to eight COVID test swabbing events in one year (approximately every 48 days) would exceed the lowest estimated cumulative exposure range of silicon for an adult of 70 kg, and the impact would be even worse for children or babies, which have been sampled even as early as 5 days from birth.[55] The toxic effects of cumulative inhalation of silica is not trivial. Death due to silicosis was

observed in 3.8% of mining and pottery workers in China, all of which were cumulatively exposed to a range of 0.1–1.23 mg/m^3/year.[56] Nanoparticles of silicon dioxide between 30 nm and 1,000 nm of diameter can induce extremely high levels of expression of the pro-inflammatory cytokine IL-1β, cause lysosomal instability, increase reactive oxygen species (ROS) levels, and lead to cell death in mouse models.[57] Actually, it has already been claimed that silica nanoparticles, commonly found in a number of commercial products used for diagnostic and therapeutic applications could be particularly toxic when inhaled.[58] Its presence in three of the analysed swab brands is compelling evidence to justify expanding our understanding of the potential biological effects of silica nanoparticles, but there is already evidence from a small number of *in vivo* studies that show mostly reversible pulmonary inflammation, granuloma formation and localized emphysema.[58]

Strontium (0.34 mg) was detected in one of the COVID test swab brands examined. It is not clear what the potential for toxicity would be for the nasal route of exposure to strontium. Most of the toxicological profiles have been determined for radioactive strontium (^{90}Sr), used for medical diagnostic procedures,[59,60] and for strontium compounds, such as strontium peroxide (SrO_2), strontium arsenite (As_2O_4Sr), strontium nitrate ($Sr(NO_3)_2$) and strontium chromate ($SrCrO_4$), where the effects are attributed to the second element, and not to strontium.[61] There is limited information regarding toxicity (LOAEL, HED) of strontium via inhalation; however, according to ATSDR,[61] the deposition of strontium particulates in the respiratory tract is dependent on the size of the inhaled particles, in addition to age, airstream speed, and airway anatomy, and, at least *in vitro*, strontium appears to impair the expression of pro-inflammatory cytokines in monocytes.[62] Regardless, it must be considered that the we are exposed daily to atmospheric strontium. In Denmark, the daily inhalation rate by exposure to atmospheric strontium (detected at an average of 5 ng Sr/m^3), which means that an adult with a body weight of 70 kg will be exposed to 175 ng of strontium from air every day.[63] Until we have more information regarding the potential effects of strontium in the upper respiratory epithelium and its biodistribution following nasopharyngeal exposure, it will simply stand as an unexpected finding in one of the COVID test swabs.

Finally, titanium and zirconium were detected in less than half of the COVID test swabs analysed, respectively, in amounts that varied from 0.22 mg to 0.45 mg. Titanium, in the form of titanium dioxide (TiO_2), and zirconium, in the form of zirconium silicate ($ZrSiO_4$) are manufactured worldwide for use in a wide range of medical, pharmaceutical and industrial applications.[64,65] Both transition metals have generally been considered as toxicologically inert. However, experimental evidence from animal inhalation studies of TiO_2 nanoparticles have shown that effects are markedly dependent on the model species,[66,67] and that in rats, TiO_2 particles elicit damage mostly via the induction of oxidative stress, which results in cell damage, genotoxicity, inflammation, and deregulated immune responses,[64,68,69] with some of the changes observable even after exposure to repeated daily doses as low as 2 ppm[70] or even 1 ppm.[71] Healthy rats exposed to concentrations of $\geq$ 2 ppm of TiO_2 particles develop alveolar macrophage sequestration, focal epithelial hypertrophic and hyperblastic proliferative changes with neutrophilic infiltration, and damage is reversible after exposure stops, as long as the dose was < 250 ppm.[67] Zirconium appears to have significantly lower toxicity than titanium.[67,72–74]

Most of our knowledge on inhalation toxicity of these transition metals derives from animal model studies, and studies on inhalation toxicity in humans are still scarce, but there have been reports of non-lethal acute intoxication following inhalation of large amounts of TiO_2,[75,76] and *in vitro* studies with human lung cell cultures have shown that there is a marked change in gene expression of cells exposed to TiO_2, with more than 2,000 genes overexpressed, including those related to ROS production.[77] Together, studies on animal models led TiO_2 nanoparticles to be classified as possibly carcinogenic to humans by the International Agency for Research on Cancer.[78] The National Institute of Occupational Safety and Health (NIOSH) recommends that the limit of aerosol exposure to TiO_2 particles be < 2.4 ppm for fine particles (1 μm–10 μm diameter) and 0.3 ppm for ultrafine particles (< 100 nm diameter), as a time-weighted average over a 10 hour day and a 40 hour work week (OSHA Fact Sheet, retrieved 17/12/2022). Given the amount of titanium and zirconium detected in the COVID test swabs, it could be argued that its presence would not be likely to cause noticeable damaging effects on the respiratory epithelium of the individuals that undergo COVID test swabbing. However, some have suggested that TiO_2 nanoparticles could exert more damage than previously thought when the compound interacts with metals and other compounds,[79] causing oxidative damage to cultured cells even at doses as low as 0.001 μg/ml.[80] This result warrants caution before dismissing the presence of titanium in COVID test swabs as concerning.

In conclusion, we identified a number of unexpected chemical elements as part of five brands of swabs used for COVID diagnostic tests. These elements can induce transient inflammation, induce cell stress, deregulate expression of cytokines and damage the epithelium following nasal exposure at doses that, at least for some of the elements detected, would be exceeded by exposure to repeated swabbing. Taking into account the lack of data on the consequences of repeated swabbing of the nasopharyngeal epithelium, and the complete absence of knowledge on the fate of micro- and nanoparticles of the elements identified herein when placed directly on the upper respiratory epithelium, their detection highlights the need for urgent studies. Under the precautionary principle, our findings warrant avoiding the recommendation of repeated testing, particularly of individuals who have no symptoms of COVID, given that, contrary to what was believed at the start of the pandemic, they play a minor epidemiological role,[81–84] particularly at this stage of the pandemic, characterized by markedly lower morbidity and mortality.[85] Having detected these unexpected and potentially toxic chemical elements leads us to propose that, rather than aiding in public health measures, unnecessary frequent swabbing of healthy individuals, could jeopardise their health. We are aware that our conclusion can be considered provocative, but we urge public health officials to consider our findings as a justification for urgent studies on the safety of repeated nasopharyngeal swabbing to be conducted, and to recommend against mandatory testing, often required for travelling, attending universities, or as mandatory work policies.

Literature cited

1. van der Elst, L. A., Gokce Kurtoglu, M., Leffel, T., Zheng, M. & Gumennik, A. Rapid Fabrication of Sterile Medical Nasopharyngeal Swabs by Stereolithography for Widespread Testing in a Pandemic. *Adv Eng Mater* **22**, 2000759 (2020).

2. Williams, E. *et al.* Pandemic printing: a novel 3D-printed swab for detecting <scp>SARS</scp> -CoV-2. *Medical Journal of Australia* **213**, 276–279 (2020).

3. Decker, S. J. *et al.* 3-Dimensional Printed Alternative to the Standard Synthetic Flocked Nasopharyngeal Swabs Used for Coronavirus Disease 2019 Testing. *Clinical Infectious Diseases* **73**, e3027–e3032 (2021).

4. Kim, C. *et al.* Comparison of Nasopharyngeal and Oropharyngeal Swabs for the Diagnosis of Eight Respiratory Viruses by Real-Time Reverse Transcription-PCR Assays. *PLoS One* **6**, e21610 (2011).

5. Scansen, K. A. *et al.* Comparison of Polyurethane Foam to Nylon Flocked Swabs for Collection of Secretions from the Anterior Nares in Performance of a Rapid Influenza Virus Antigen Test in a Pediatric Emergency Department. *J Clin Microbiol* **48**, 852–856 (2010).

6. Verdon, T. J., Mitchell, R. J. & van Oorschot, R. A. H. Swabs as DNA Collection Devices for Sampling Different Biological Materials from Different Substrates. *J Forensic Sci* **59**, 1080–1089 (2014).

7. Bolaños-Suaréz, V. *et al.* Validation of 3D-Printed Swabs for Sampling in SARS-CoV-2 Detection: A Pilot Study. *Ann Biomed Eng* (2022) doi:10.1007/s10439-022-03057-1.

8. Zasada, A. A. *et al.* The influence of a swab type on the results of point-of-care tests. *AMB Express* **10**, 46 (2020).

9. McCarthy, A. *et al.* Ultra-absorptive Nanofiber Swabs for Improved Collection and Test Sensitivity of SARS-CoV-2 and other Biological Specimens. *Nano Lett* **21**, 1508–1516 (2021).

10. Kashapov, R. N. & Tsibin, A. N. Comparison of the Physical Properties and Effectiveness of Medical Swabs for Sampling Biomaterials. *Biomed Eng (NY)* **55**, 289–293 (2021).

11. Kim, C. *et al.* Comparison of Nasopharyngeal and Oropharyngeal Swabs for the Diagnosis of Eight Respiratory Viruses by Real-Time Reverse Transcription-PCR Assays. *PLoS One* **6**, e21610 (2011).

12. Vashist, V., Banthia, N., Kumar, S. & Agrawal, P. A systematic review on materials, design, and manufacturing of swabs. *Annals of 3D Printed Medicine* **9**, 100092 (2023).

13. Gupta, K., Bellino, P. M. & Charness, M. E. Adverse effects of nasopharyngeal swabs: Three-dimensional printed versus commercial swabs. *Infect Control Hosp Epidemiol* **42**, 641–642 (2021).

14. Koskinen, A. *et al.* Complications of COVID-19 Nasopharyngeal Swab Test. *JAMA Otolaryngology–Head & Neck Surgery* **147**, 672 (2021).

15. Sullivan, C. B. *et al.* Cerebrospinal Fluid Leak After Nasal Swab Testing for Coronavirus Disease 2019. *JAMA Otolaryngology–Head & Neck Surgery* **146**, 1179 (2020).

16. Föh, B. *et al.* Complications of nasal and pharyngeal swabs: a relevant challenge of the COVID-19 pandemic? *European Respiratory Journal* **57**, 2004004 (2021).

17. Fazekas, B., Fazekas, B., Darraj, E. & Jayakumar, D. Preseptal cellulitis and infraorbital abscess as a complication of a routine COVID-19 swab. *BMJ Case Rep* **14**, e241963 (2021).

18. Kim, D. H., Kim, D., Moon, J. W., Chae, S.-W. & Rhyu, I. J. Complications of Nasopharyngeal Swabs and Safe Procedures for COVID-19 Testing Based on Anatomical Knowledge. *J Korean Med Sci* **37**, (2022).

19. Alberola-Amores, F. J., Valdeolivas-Urbelz, E., Torregrosa-Ortiz, M., Álvarez-Sauco, M. & Alom-Poveda, J. Meningitis due to cerebrospinal fluid leak after nasal swab testing for COVID-19. *Eur J Neurol* **28**, (2021).

20. Krupińska, M. *et al.* Wild Red Deer (Cervus elaphus) Do Not Play a Role as Vectors or Reservoirs of SARS-CoV-2 in North-Eastern Poland. *Viruses* **14**, 2290 (2022).

21. Hamdy, M. E. *et al.* SARS-CoV-2 infection of companion animals in Egypt and its risk of spillover. *Vet Med Sci* (2022) doi:10.1002/vms3.1029.

22. Sangkachai, N. *et al.* Serological and Molecular Surveillance for SARS-CoV-2 Infection in Captive Tigers (Panthera tigris), Thailand. *Animals* **12**, 3350 (2022).

23. Taheraslani, M., Gardeniers, H. High-Resolution SEM and EDX Characterization of Deposits Formed by CH4+Ar DBD Plasma Processing in a Packed Bed Reactor. *Nanomaterials* **9**, 589 (2019). doi: 10.3390/nano9040589

24. Shi, B., Topolkaraev, V. & Wang, J. Biopolymers, Processing, and Biodegradation. in 117–132 (2011). doi:10.1021/bk-2011-1063.ch008.

25. Darie-Niță, R. N., Râpă, M. & Frąckowiak, S. Special Features of Polyester-Based Materials for Medical Applications. *Polymers (Basel)* **14**, 951 (2022).

26. DEOPURA, B. L. Polyamide fibers. in *Polyesters and Polyamides* 41–61 (Elsevier, 2008). doi:10.1533/9781845694609.1.41.

27. Das, A. & Mahanwar, P. A brief discussion on advances in polyurethane applications. *Advanced Industrial and Engineering Polymer Research* **3**, 93–101 (2020).

28. Costa, N. *et al.* Physical, Chemical, and Immunohistochemical Investigation of the Damage to Salivary Glands in a Model of Intoxication with Aluminium Citrate. *Int J Environ Res Public Health* **11**, 12429–12440 (2014).

29. Peto, M. v. Aluminium and Iron in Humans: Bioaccumulation, Pathology, and Removal. *Rejuvenation Res* **13**, 589–598 (2010).

30. Aguirre-Sierra, A., Alonso, Á. & Camargo, J. A. Fluoride Bioaccumulation and Toxic Effects on the Survival and Behavior of the Endangered White-Clawed Crayfish

Austropotamobius pallipes (Lereboullet). *Arch Environ Contam Toxicol* **65**, 244–250 (2013).

31. Johnston, N. R. & Strobel, S. A. Principles of fluoride toxicity and the cellular response: a review. *Arch Toxicol* **94**, 1051–1069 (2020).

32. Novaes, R. D. *et al.* Aluminum: A potentially toxic metal with dose-dependent effects on cardiac bioaccumulation, mineral distribution, DNA oxidation and microstructural remodeling. *Environmental Pollution* **242**, 814–826 (2018).

33. Tuncsoy, B. & Mese, Y. Influence of titanium dioxide nanoparticles on bioaccumulation, antioxidant defense and immune system of Galleria mellonella L. *Environmental Science and Pollution Research* **28**, 38007–38015 (2021).

34. Marisa, I. *et al.* Bioaccumulation and effects of titanium dioxide nanoparticles and bulk in the clam *Ruditapes philippinarum*. *Mar Environ Res* **136**, 179–189 (2018).

35. Bourgeault, A. *et al.* The Challenge of Studying TiO_2 Nanoparticle Bioaccumulation at Environmental Concentrations: Crucial Use of a Stable Isotope Tracer. *Environ Sci Technol* **49**, 2451–2459 (2015).

36. Kumar, S. *et al.* Biofunctionalized Nanostructured Zirconia for Biomedical Application: A Smart Approach for Oral Cancer Detection. *Advanced Science* **2**, 1500048 (2015).

37. Wang, R. *et al.* Wear behavior of light-cured resin composites with bimodal silica nanostructures as fillers. *Materials Science and Engineering: C* **33**, 4759–4766 (2013).

38. Sajtos, Z. *et al.* The retention of Zr from potential therapeutic silica-zirconia core–shell nanoparticles in aquatic organisms. *Environ Nanotechnol Monit Manag* **16**, 100572 (2021).

39. Tang, L. & Cheng, J. Nonporous silica nanoparticles for nanomedicine application. *Nano Today* **8**, 290–312 (2013).

40. Vivero-Escoto, J. L., Huxford-Phillips, R. C. & Lin, W. Silica-based nanoprobes for biomedical imaging and theranostic applications. *Chem Soc Rev* **41**, 2673 (2012).

41. Douroumis, D., Onyesom, I., Maniruzzaman, M. & Mitchell, J. Mesoporous silica nanoparticles in nanotechnology. *Crit Rev Biotechnol* **33**, 229–245 (2013).

42. Duan, J. *et al.* Toxic Effects of Silica Nanoparticles on Zebrafish Embryos and Larvae. *PLoS One* **8**, e74606 (2013).

43. Athanassiou, C. G. *et al.* Nanoparticles for pest control: current status and future perspectives. *J Pest Sci (2004)* **91**, 1–15 (2018).

44. ATSDR. *Toxicological profile for fluorides, hydrogen fluoride, and fluorine*. (2003).

45. Zuo, H. *et al.* Toxic effects of fluoride on organisms. *Life Sci* **198**, 18–24 (2018).

46. Bartos, M. *et al.* Rat developmental fluoride exposure affects retention memory, leads to a depressive-like behavior, and induces biochemical changes in offspring rat brains. *Neurotoxicology* **93**, 222–232 (2022).

47. ATSDR. *Toxicological profile for Aluminum*. (2008).

48. Chalansonnet, M. *et al.* Study of potential transfer of aluminum to the brain via the olfactory pathway. *Toxicol Lett* **283**, 77–85 (2018).

49. Kwon, J.-T. *et al.* Pulmonary Toxicity Assessment of Aluminum Oxide Nanoparticles via Nasal Instillation Exposure. *Korean Journal of Environmental Health Sciences* **39**, 48–55 (2013).

50. Krewski, D. *et al.* Human Health Risk Assessment for Aluminium, Aluminium Oxide, and Aluminium Hydroxide. *Journal of Toxicology and Environmental Health, Part B* **10**, 1–269 (2007).

51. Polyzois, I., Nikolopoulos, D., Michos, I., Patsouris, E. & Theocharis, S. Local and systemic toxicity of nanoscale debris particles in total hip arthroplasty. *Journal of Applied Toxicology* **32**, 255–269 (2012).

52. Elsabahy, M. & Wooley, K. L. Cytokines as biomarkers of nanoparticle immunotoxicity. *Chem Soc Rev* **42**, 5552 (2013).

53. Sasaki, E. *et al.* Nasal alum-adjuvanted vaccine promotes IL-33 release from alveolar epithelial cells that elicits IgA production via type 2 immune responses. *PLoS Pathog* **17**, e1009890 (2021).

54. Steenland, K. & Brown, D. Silicosis among gold miners: exposure--response analyses and risk assessment. *Am J Public Health* **85**, 1372–1377 (1995).

55. Rood, M., ten Kate, L., Boeddha, N. P. & van ‘t Kruys, K. Clinical Characteristics, Transmission Rate and Outcome of Neonates Born to COVID-19-Positive Mothers: A Prospective Case Series From a Resource-Limited Setting. *Pediatric Infectious Disease Journal* **42**, 35–42 (2023).

56. Chen, M. & Tse, L. A. Laryngeal cancer and silica dust exposure: A systematic review and meta-analysis. *Am J Ind Med* **55**, 669–676 (2012).

57. Kusaka, T. *et al.* Effect of Silica Particle Size on Macrophage Inflammatory Responses. *PLoS One* **9**, e92634 (2014).

58. Napierska, D., Thomassen, L. C., Lison, D., Martens, J. A. & Hoet, P. H. The nanosilica hazard: another variable entity. *Part Fibre Toxicol* **7**, 39 (2010).

59. Reissig, F., Kopka, K. & Mamat, C. The impact of barium isotopes in radiopharmacy and nuclear medicine – From past to presence. *Nucl Med Biol* **98–99**, 59–68 (2021).

60. Gillett, N. A. *et al.* Single inhalation exposure to 90SrCl2 in the beagle dog: late biological effects. *J Natl Cancer Inst* **79**, 359–76 (1987).

61. ASTDR. *Toxicological profile for strontium*. (2004).

62. Buache, E. *et al.* Effect of strontium-substituted biphasic calcium phosphate on inflammatory mediators production by human monocytes. *Acta Biomater* **8**, 3113–3119 (2012).

63. Nielsen, E., Greve, K. & Ladefoged, O. *Strontium, inorganic and soluble salts. Evaluation of health hazards and proposal of health based quality criteria for drinking water*. (2008).

64. Hext, P. M., Tomenson, J. A. & Thompson, P. Titanium Dioxide: Inhalation Toxicology and Epidemiology. *Ann Occup Hyg* **49**, 461–472 (2005).

65. Zirconium and its compounds [MAK Value Documentation, 1999]. in *The MAK-Collection for Occupational Health and Safety* 224–236 (Wiley-VCH Verlag GmbH & Co. KGaA, 2012). doi:10.1002/3527600418.mb744067vere0012.

66. Bermudez, E. Long-Term Pulmonary Responses of Three Laboratory Rodent Species to Subchronic Inhalation of Pigmentary Titanium Dioxide Particles. *Toxicological Sciences* **70**, 86–97 (2002).

67. Hext, P. M. *et al.* Comparison of the Pulmonary Responses to Inhaled Pigmentary and Ultrafine Titanium Dioxide Particles in the Rat, Mouse and Hamster. *Ann Occup Hyg* (2002) doi:10.1093/annhyg/46.suppl_1.191.

68. PetkoviĆ, J. *et al.* DNA damage and alterations in expression of DNA damage responsive genes induced by TiO_2 nanoparticles in human hepatoma HepG2 cells. *Nanotoxicology* **5**, 341–353 (2011).

69. Ahn, M.-H. *et al.* Titanium dioxide particle – induced goblet cell hyperplasia : association with mast cells and IL-13. *Respir Res* **6**, 34 (2005).

70. Rossi, E. M. *et al.* Inhalation exposure to nanosized and fine TiO2 particles inhibits features of allergic asthma in a murine model. *Part Fibre Toxicol* **7**, 35 (2010).

71. Chen, H. *et al.* Titanium dioxide nanoparticles induce emphysema-like lung injury in mice. *The FASEB Journal* **20**, 2393–2395 (2006).

72. Ramenzoni, L. L., Flückiger, L. B., Attin, T. & Schmidlin, P. R. Effect of Titanium and Zirconium Oxide Microparticles on Pro-Inflammatory Response in Human Macrophages under Induced Sterile Inflammation: An In Vitro Study. *Materials* **14**, 4166 (2021).

73. Schwarz, F. *et al.* Cytotoxicity and proinflammatory effects of titanium and zirconia particles. *Int J Implant Dent* **5**, 25 (2019).

74. Obando-Pereda, G. A., Fischer, L. & Stach-Machado, D. R. Titanium and zirconia particle-induced pro-inflammatory gene expression in cultured macrophages and osteolysis, inflammatory hyperalgesia and edema in vivo. *Life Sci* **97**, 96–106 (2014).

75. Ahmadimanesh, M., Shadnia, S. & Ghazi-Khansari, M. Acute inhalation exposure to titanium ethanolate as a possible cause of metal fume fever. *Int J Occup Environ Med* **5**, 106–8 (2014).

76. Otani, N., Ishimatsu, S. & Mochizuki, T. Acute group poisoning by titanium dioxide: inhalation exposure may cause metal fume fever. *Am J Emerg Med* **26**, 608–611 (2008).

77. Jayaram, D. T. *et al.* TiO_2 nanoparticles generate superoxide and alter gene expression in human lung cells. *RSC Adv* **9**, 25039–25047 (2019).

78. Baan, R. A. Carcinogenic Hazards from Inhaled Carbon Black, Titanium Dioxide, and Talc not Containing Asbestos or Asbestiform Fibers: Recent Evaluations by an *IARC Monographs* Working Group. *Inhal Toxicol* **19**, 213–228 (2007).

79. Liu, K., Lin, X. & Zhao, J. Toxic effects of the interaction of titanium dioxide nanoparticles with chemicals or physical factors. *Int J Nanomedicine* 2509 (2013) doi:10.2147/IJN.S46919.

80. Du, H. *et al.* Oxidative damage and OGG1 expression induced by a combined effect of titanium dioxide nanoparticles and lead acetate in human hepatocytes. *Environ Toxicol* **27**, 590–597 (2012).

81. Muller, C. P. Do asymptomatic carriers of SARS-COV-2 transmit the virus? *The Lancet Regional Health - Europe* **4**, 100082 (2021).

82. Methi, F. & Madslien, E. H. Lower transmissibility of SARS-CoV-2 among asymptomatic cases: evidence from contact tracing data in Oslo, Norway. *BMC Med* **20**, 427 (2022).

83. He, D. *et al.* The relative transmissibility of asymptomatic COVID-19 infections among close contacts. *International Journal of Infectious Diseases* **94**, 145–147 (2020).

84. Cao, S. *et al.* Post-lockdown SARS-CoV-2 nucleic acid screening in nearly ten million residents of Wuhan, China. *Nat Commun* **11**, 5917 (2020).

85. Pezullo, A. M. et al. Age-stratified infection fatality rate of COVID-19 in the non-elderly population. *Environ Res* **216**, 114655 (2023).

Author contributions: MAA and KAW conceived the study, VTS prepared the samples for SEM and EDX analysis and wrote the first draft of the paper, FCM analysed the EDX results. All authors contributed to the discussion of the results.

Data availability statement: Data on EDX results and element profiles is available in the Supplementary Materials information. Any other data relevant to the manuscript can be requested from the corresponding authors.

Competing Interests Statement: The author(s) declare no competing interests.

Figure legends

Figure 1. Scanning electron micrographs of different materials and structures of A) foam swab (iHealth), B) nylon-flocked swab (Puritan), C) nylon-flocked swab (CM LAB), D) nylon swab (Miraclean), E) nylon swab (COPAN), F) cotton swab used for generic applications (DM Productora) and G) cotton swab used for bacterial transport (COPAN). Magnification was 300 X except for panel A, which is 100X.

Scanning electron microscopy and EDX spectroscopy of commercial swabs used for COVID-19 lateral flow testing

Manuel Aparicio-Alonso, Verónica Torres-Solórzano, José Francisco Méndez Contreras, Karina Acevedo-Whitehouse

Supplementary figures

The next figures show, for each of the five COVID swab test brands analysed, the scanning electron micrographs and XED spectroscopy element analysis. The Supplementary Figures are presented in the following order:

Supplementary Figure	Brand	Fabric	CE	Manufacturer	Lot number
1	iHealth®	Foam	No	iHealth Labs,Inc	20211213
2	Puritan HydraFlock®	Nylon flocked	Yes	Puritan Med Products	(10) 50173
3	Nasal Swab	Nylon flocked	Yes	CM LAB SAS	20201221
4	MANTACC®	Nylon	Yes	Miraclean Technology Co., Ltd	2021120864
5	FLOQSwabs ®	Nylon	Yes	COPAN	2010482

CE, Conformité Européenne

Scanning electron microscopy and EDX spectroscopy of commercial swabs used for COVID-19 lateral flow testing (Aparicio-Alonso, M, Torres-Solórzano, V, Méndez Contreras JF, Acevedo-Whitehouse, K)

SUPPLEMENTARY FIGURES

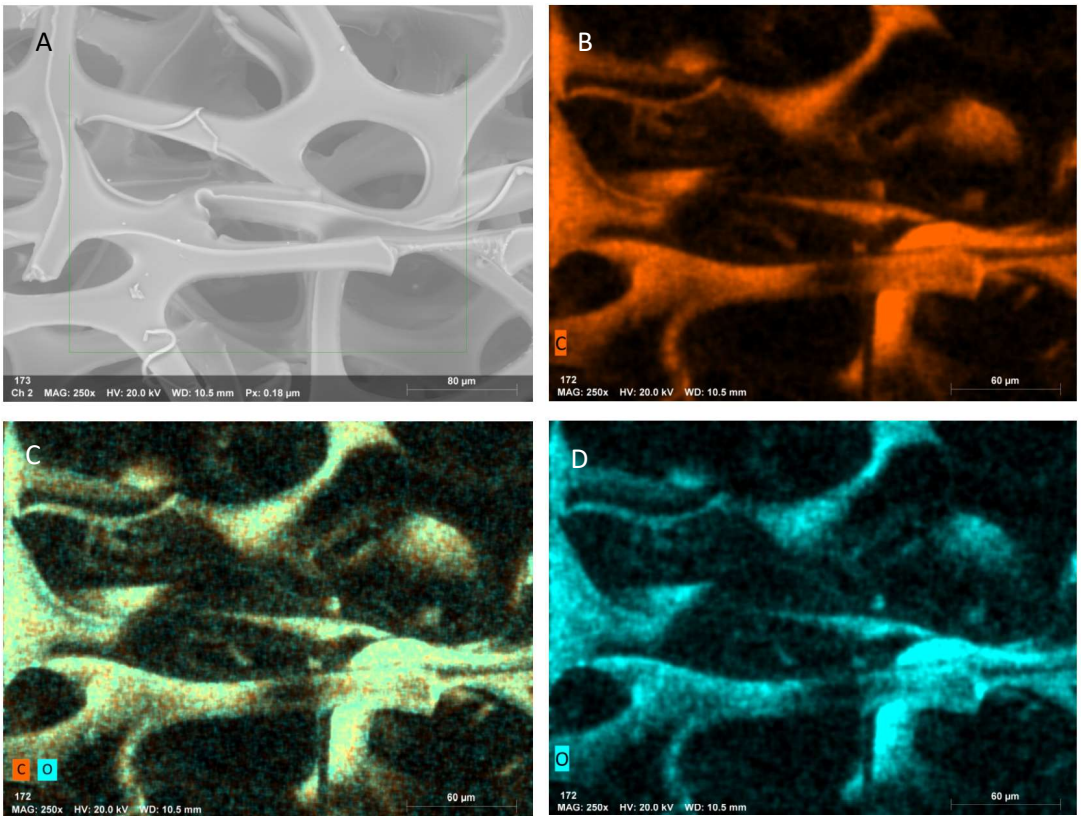

E

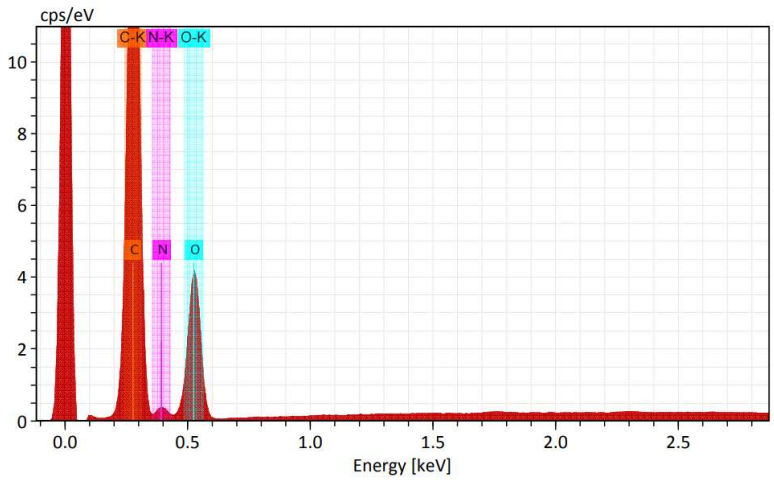

Map

Element	At. No.	Netto	Mass [%]	Mass Norm. [%]	Atom [%]	abs. error [%] (1 sigma)	rel. error [%] (1 sigma)
Carbon	6	338921	57.99	58.27	64.42	6.22	10.73
Nitrogen	7	7919	8.02	8.06	7.64	1.19	14.81
Oxygen	8	85453	33.51	33.67	27.94	3.83	11.44
		Sum	**99.52**	**100.00**	**100.00**		

Figure S1. Analysis of swab 1 (foam head; brand: iHealth). A) Scanning electron micrograph of swab head; B) Distribution of Carbon; C) Distribution of Carbon and Oxygen; D) Distribution of Oxygen; E) Chemical elements identified by EDX spectroscopy.

Scanning electron microscopy and EDX spectroscopy of commercial swabs used for COVID-19 lateral flow testing (Aparicio-Alonso, M, Torres-Solórzano, V, Méndez Contreras JF, Acevedo-Whitehouse, K)

SUPPLEMENTARY FIGURES

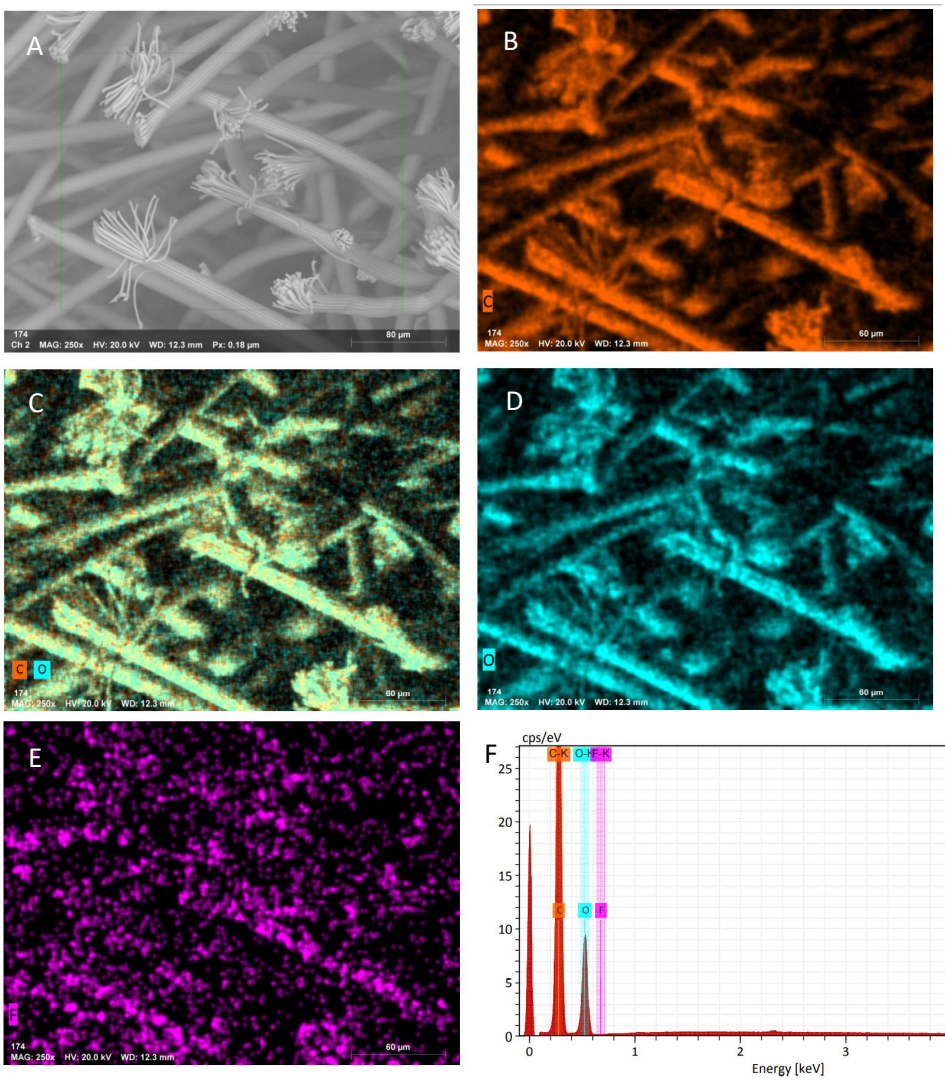

Map

Element	At. No.	Netto	Mass [%]	Mass Norm. [%]	Atom [%]	abs. error [%] (1 sigma)	rel. error [%] (1 sigma)
Carbon	6	392974	62.43	62.66	69.14	6.67	10.68
Oxygen	8	112032	36.69	36.82	30.50	4.13	11.26
Fluorine	9	1665	0.52	0.52	0.37	0.13	24.59
		Sum	**99.64**	**100.00**	**100.00**		

Figure S2. Analysis of swab 2 (nylon flocked head; brand: Puritan HydraFlock). A) Scanning electron micrograph of swab head; B) Distribution of Carbon; C) Distribution of Carbon and Oxygen; D) Distribution of Oxygen; E) Distribution of Fluorine; F) Chemical elements identified by EDX spectroscopy.

Scanning electron microscopy and EDX spectroscopy of commercial swabs used for COVID-19 lateral flow testing (Aparicio-Alonso, M, Torres-Solórzano, V, Méndez Contreras JF, Acevedo-Whitehouse, K)

SUPPLEMENTARY FIGURES

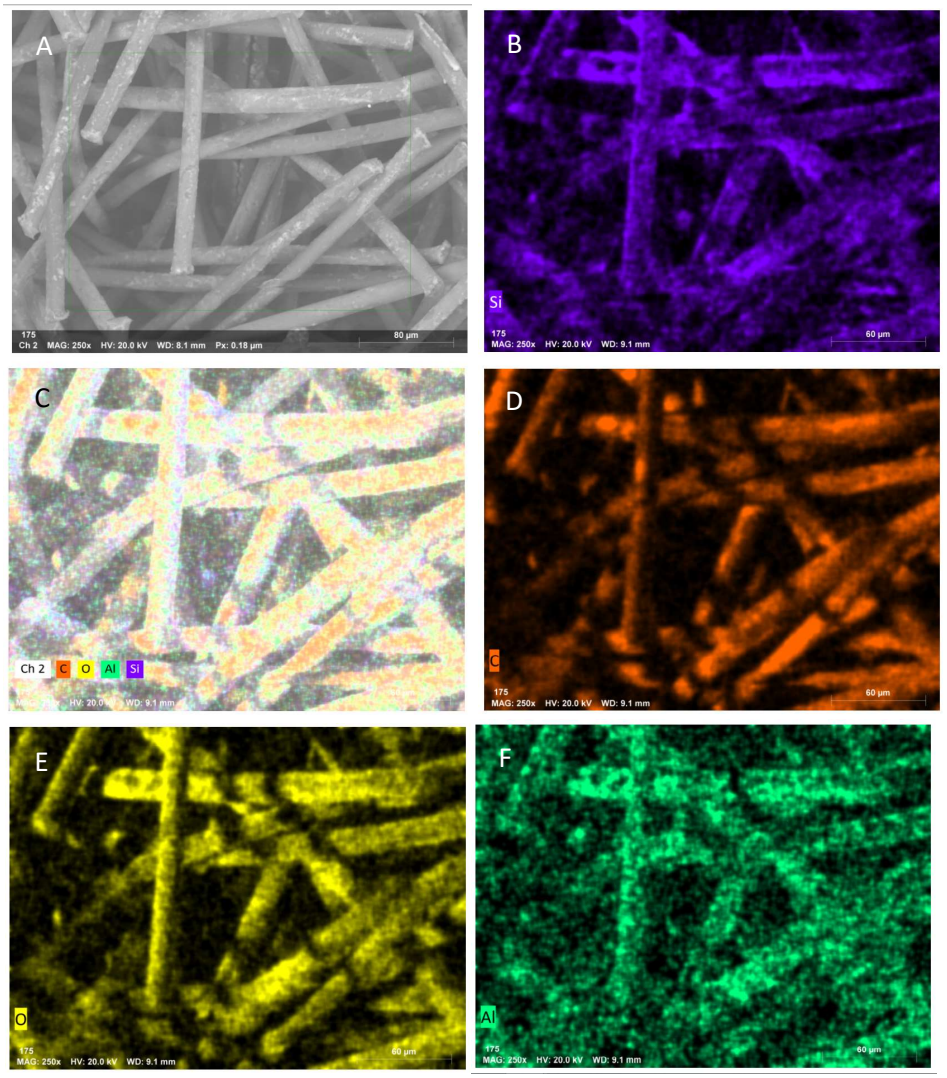

Map

Element	At. No.	Netto	Mass [%]	Mass Norm. [%]	Atom [%]	abs. error [%] (1 sigma)	rel. error [%] (1 sigma)
Carbon	6	207987	53.13	53.49	61.26	5.80	10.92
Nitrogen	7	4714	4.83	4.86	4.78	0.79	16.34
Oxygen	8	96529	36.04	36.29	31.20	4.09	11.36
Fluorine	9	1489	0.53	0.53	0.38	0.13	25.13
Aluminium	13	13154	0.62	0.62	0.32	0.06	9.01
Silicon	14	114757	4.18	4.21	2.06	0.20	4.87
		Sum	**99.32**	**100.00**	**100.00**		

Figure S3. Analysis of swab 3 (nylon flocked head; brand: Nasal Swab). A) Scanning electron micrograph of swab head; B) Distribution of Silicon; C) Distribution of Carbon, Oxygen, Aluminium, Silicon; D) Distribution of Carbon; E) Distribution of Oxygen; F) Distribution of Aluminium; G) Chemical elements identified by EDX

Scanning electron microscopy and EDX spectroscopy of commercial swabs used for COVID-19 lateral flow testing (Aparicio-Alonso, M, Torres-Solórzano, V, Méndez Contreras JF, Acevedo-Whitehouse, K)

SUPPLEMENTARY FIGURES

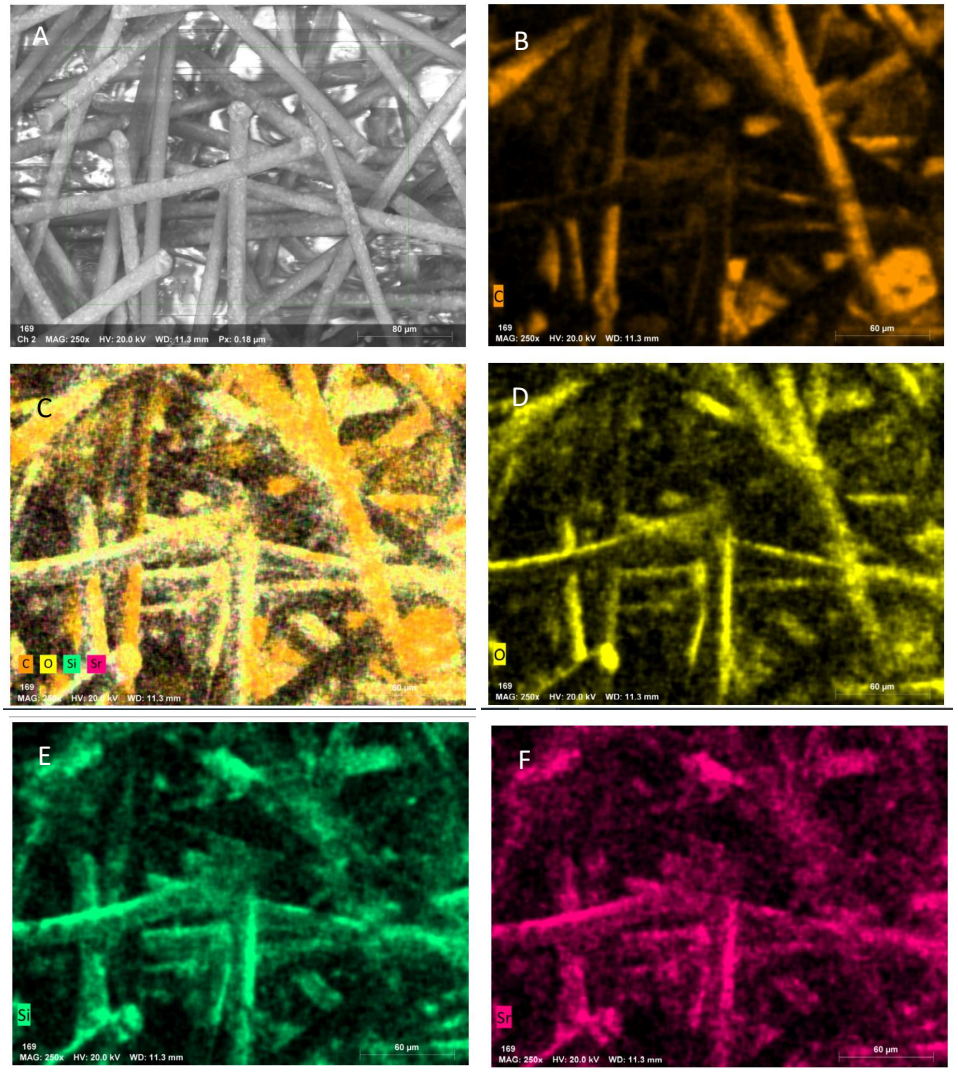

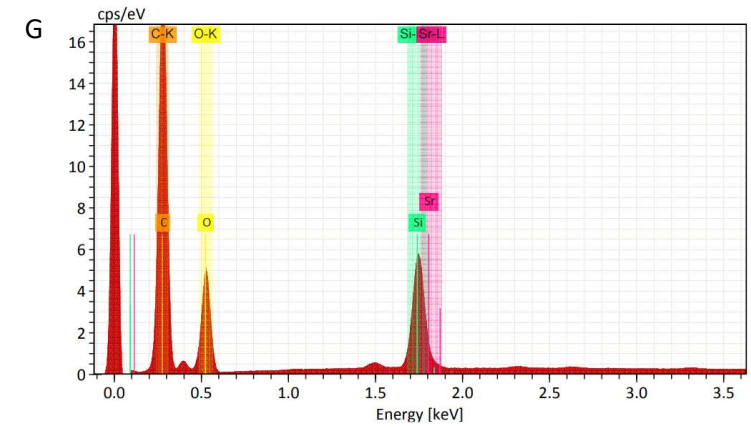

Map

Element	At. No.	Netto	Mass [%]	Mass Norm. [%]	Atom [%]	abs. error [%] (1 sigma)	rel. error [%] (1 sigma)
Carbon	6	329608	59.60	60.19	68.08	6.40	10.74
Nitrogen	7	5644	4.75	4.80	4.66	0.75	15.85
Oxygen	8	93964	29.22	29.51	25.05	3.33	11.39
Silicon	14	146188	3.79	3.83	1.85	0.19	4.93
Titanium	22	18324	0.78	0.79	0.22	0.05	6.09
Strontium	38	16740	0.87	0.88	0.14	0.06	7.11
		Sum	**99.02**	**100.00**	**100.00**		

Figure S4. Analysis of swab 4 (nylon head; brand: MANTACC). A) Scanning electron micrograph of swab head; B) Distribution of Carbon; C) Distribution of Carbon, Oxygen, Silicon, Strontium; D) Distribution of Oxygen; E) Distribution of Silicon; F) Distribution of Strontium; G) Chemical elements identified by EDX spectroscopy.

Scanning electron microscopy and EDX spectroscopy of commercial swabs used for COVID-19 lateral flow testing (Aparicio-Alonso, M, Torres-Solórzano, V, Méndez Contreras JF, Acevedo-Whitehouse, K)

SUPPLEMENTARY FIGURES

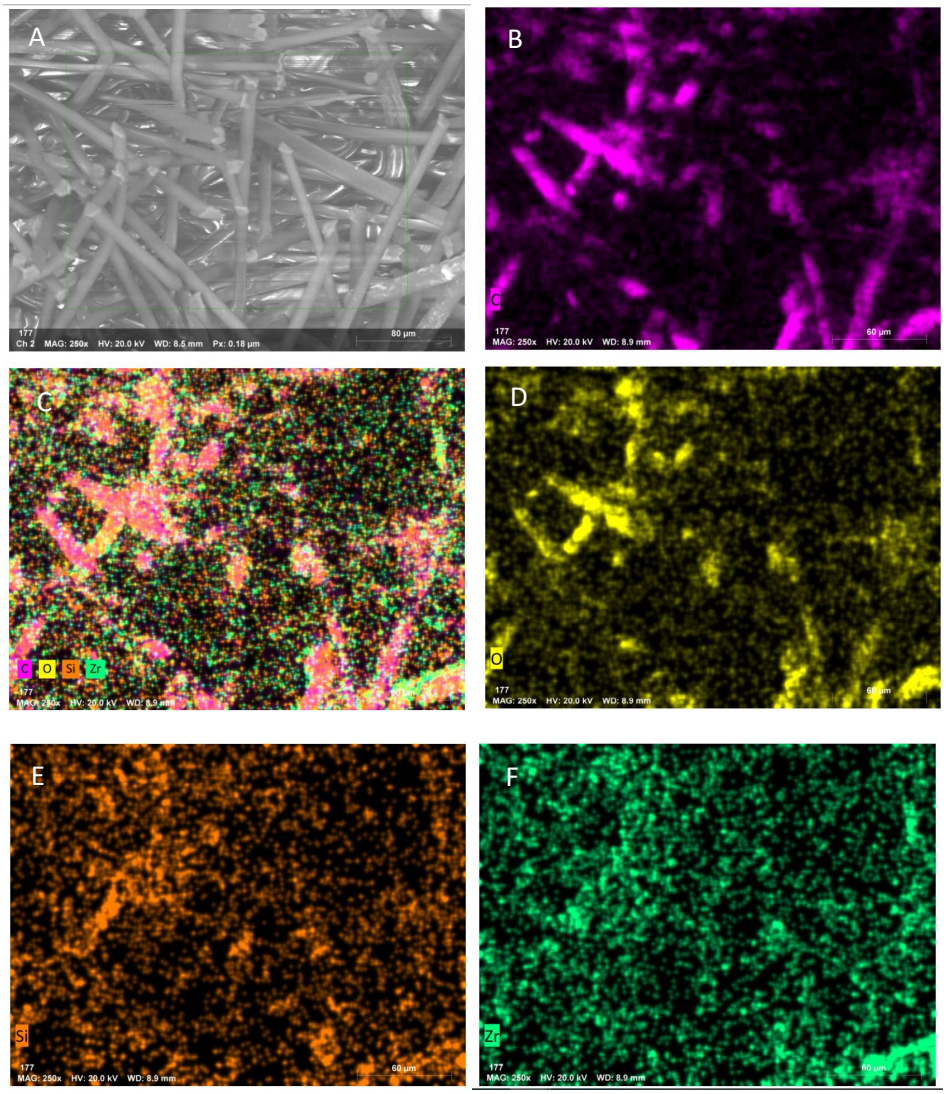

Map

Element	At. No.	Netto	Mass [%]	Mass Norm. [%]	Atom [%]	abs. error [%] (1 sigma)	rel. error [%] (1 sigma)
Carbon	6	95535	63.84	64.04	70.44	7.24	11.33
Nitrogen	7	2488	10.26	10.29	9.70	1.87	18.26
Oxygen	8	13758	23.24	23.31	19.25	3.14	13.52
Silicon	14	3630	0.54	0.55	0.26	0.05	9.44
Titanium	22	3464	0.60	0.60	0.17	0.05	7.55
Zirconium	40	4909	1.21	1.21	0.18	0.08	6.31
		Sum	**99.70**	**100.00**	**100.00**		

Figure S5. Analysis of swab 5 (nylon flocked head; brand: FLOQSwabs). A) Scanning electron micrograph of swab head; B) Distribution of Carbon; C) Distribution of Carbon, Oxygen, Silicon, Zirconium; D) Distribution of Oxygen; E) Distribution of Silicon; F) Distribution of Zirconium; G) Chemical elements identified by EDX spectroscopy.